Rotational Magnetization Processes in Meso- and Nanoscopic Magnets

Josef Fidler, Thomas Schrefl, Werner Scholz and Dieter Suess

Vienna University of Technology
Institute of Applied and Technical Physics,
Wiedner Hauptstr. 8-14, A-1040 Wien, Austria.
fidler@tuwien.ac.at

Abstract

Traditional investigations of the magnetization reversal in small ferromagnetic particles assume spherical or ellipsoidal particles uniformly magnetized along the easy direction in the ramanent state. The reversal mechanism in nonellipsoidal particles have been rigorously studied applying finite difference or finite element techniques. The numerical results clearly show that strong stray fields, which cause the magnetization to become inhomogeneously arranged, influence the reversal process drastically. Micromagnetic modelling of the magnetization reversal process of meso- and nanoscopic magnetic elements which are patterned structures at the submicron level show that the shape and size of cubic, disc and platelet elements become an important factor controlling the incoherent rotational magnetization processes. A finite element method was used to simulate the magnetization reversal of nanostructured Co and $Ni_{80}Fe_{20}$ elements. The numerical results show a strong influence of the size of the cubic and platelet shaped (square and triangular) elements on the switching field. The calculated switching fields range from $\mu_0 H$=0.002 to 0.6 T. Differences of the demagnetizing field which arise when the field is applied in different directions, lead to configurational anisotropy effects. Platelet shaped elements show identical switching behaviour in different directions within the platelet plane. Inhomogeneous magnetization reversal processes become dominant with increasing element size $\geq$ 100 nm and strongly influence the switching behaviour. The numerical results show that the Gilbert damping constant, α, which was varied between 0.1 and 0.02 drastically changes the reversal mode. The switching fields and times which are in the order of nano- or picoseconds can be varied by the choice of the geometric shape of the magnets, the intrinsic properties and the orientation and strength of the applied field. Micromagnetic modelling of the show that the dynamics of the switching behaviour in a reversed field differs from the one in a rotating field, especially at high frequencies in the GHz range.

Introduction

Nanofabrication, offering unprecedented capabilities in the manipulation of material structures and properties, opens up new opportunities for engineering innovative magnetic materials and devices, developing ultra-high-density magnetic storage. The reduced grain size considerably increases the storage density of high density magneto-optical and longitudinal recording media [1,2]. Nanoscale Ni-Fe and Co patterned media are able to achieve recording densities higher than 100 Gbits/inch^2 [3]. The increasing information density in magnetic recording, the miniaturization in magnetic sensor technology, the trend towards nanocrystalline magnetic materials and the improved availability of large scale computer power are the main reasons why micromagnetic modelling has been developing extremely rapidly. Computational micromagnetism leads to a deeper understanding of hysteresis effects by visualization of the magnetization reversal process of mesoscopic and nanoscopic magnetic structures. The micromagnetic theory is an approach to explain the magnetization reversal or hysteresis effects of ferro- and ferrimagnetic materials at an intermediate length scale between magnetic domains and crystal lattice sites. Micromagnetism is a generic term used for a wide variety of studies of magnetization structures and reversal mechanisms in magnetic materials. Numerical

micromagnetic modelling using the finite difference or finite element method reveals the correlation between the local arrangement of the magnetic moments and the microstructural features on a length scale of several nanometers. Computational micromagnetics gives a quantitative treatment of the influence of the microstructure and shape of the magnet device on the magnetization reversal and hysteresis processes.

Traditional investigations of magnetization reversal in small ferromagnetic particles assume spherical or ellipsoidal particles uniformly magnetized along the easy direction for zero applied field. At the nucleation field the magnetization starts to deviate from the equilibrium state according to the preferred magnetization mode [4,5]. The magnetization reversal mechanism in nonellipsoidal particles have been rigorously studied applying finite difference [6,7] or finite element techniques [8]. The numerical results clearly show that strong stray fields, which cause the magnetization to become inhomogeneously arranged, influence the reversal process drastically [9-11]. Owing to stray field effects the angular dependence of the nucleation field of nonellipsoidal particles considerably deviates from the classical results [12]. We developed a new numerical procedure to study static and dynamic behaviour in micromagnetic systems. This procedure solves the damped Gilbert equation for a continuous magnetic medium, including all interactions in standard micromagnetic theory in three-dimensional regions of arbitrary geometry, polycrystalline grain structure and physical properties. This paper reviews recent results in numerical micromagnetic 3D-simulations of the magnetic switching dynamics and shows the differences occurring, if uniaxial reversed fields or rotational fields are applied to single crystalline NiFe- and Co-elements with various geometries and sizes.

Micromagnetic and numerical concept

Micromagnetism starts from the total magnetic Gibb's free energy, E_t, of a ferromagnetic system, which is the sum of the exchange energy, the Zeeman energy, the magnetostatic energy and the magneto-crystalline anisotropy energy [13]. Minimising E_t with respect to the magnetization yields a stable equilibrium state of the magnetic structure. All energy terms but the stray field energy depend only locally on the magnetization. Thus the direct evaluation of the total magnetic Gibb's free energy requires both large memory space and long computation time. The magnetostatic field is a long-range interaction whose calculation is the most time-consuming part of the micromagnetic problem. Introducing a magnetic vector potential to treat the demagnetising field eliminates long-range interactions from the total magnetic Gibb's free energy [14]. This leads to a sparse, algebraic minimisation problem. Since the magnetic polarization **J** and the magnetic vector potential **A** are independent variables, the minimisation can be performed simultaneously with respect to **J** and **A**. Alternatively, it is possible to introduce a magnetic scalar potential Ψ to compute the demagnetising field. The energy functional is free from any long-range term leading to effective numerical algorithms that require only limited memory. Starting from the vector of the magnetic polarization as a function of space and time leads to a standard total free energy expression for a system within a certain volume:

$$E_t(\mathbf{J},\mathbf{A}) = \int \left[\frac{A}{J_s^2}(\nabla \mathbf{J})^2 - K_1\left(\mathbf{u}_c \cdot \frac{\mathbf{J}}{J_s}\right)^2 - \mathbf{J}\cdot\mathbf{H}_{ext} + \frac{1}{2\mu_0}(\nabla\times\mathbf{A}-\mathbf{J})^2 \right] dV \qquad (1)$$

or

$$E_t(\mathbf{J},\Psi) = \int \left[\frac{A}{J_s^2}(\nabla \mathbf{J})^2 - K_1\left(\mathbf{u}_c \cdot \frac{\mathbf{J}}{J_s}\right)^2 - \mathbf{J}\cdot\mathbf{H}_{ext} - \mathbf{J}\cdot\nabla\Psi \right] dV \qquad (2)$$

with the constraint

$$\Delta\Psi = -\frac{1}{\mu_0}\nabla\mathbf{J} \qquad (3)$$

The temperature dependent constants J_s, A, K_1 are the saturation polarization, the exchange constant and the magnetocrystalline anisotropy constant, respectively. The first term of the total energy expression is the exchange energy, followed by the magnetocrystalline anisotropy energy for uniaxial systems with the easy axis direction $\mathbf{u}_c$, the Zeeman coupling to an external magnetic field Hext and the stray field energy arising from magnetic dipole interactions. The last term is the most severe problem to be solved.

From the thermodynamical principle of irreversibility the equation of motion for the magnetic polarization was derived by Landau and Lifshitz [15]

$$\frac{\partial \mathbf{J}}{\partial t} = -\frac{|\gamma|}{1+\alpha^2}\left(\mathbf{J}\times\mathbf{H}_{\text{eff}}\right) - \frac{\alpha}{J_s\cdot\left(1+\alpha^2\right)}\left[\mathbf{J}\times\left(\mathbf{J}\times\mathbf{H}_{\text{eff}}\right)\right] \qquad (4)$$

with

$$\mathbf{H}_{\text{eff}} = -\frac{\delta E_t}{\delta \mathbf{J}} \qquad (5)$$

or in the equivalent form given by Gilbert [16]

$$\frac{\partial \mathbf{J}}{\partial t} = -|\gamma|\left(\mathbf{J}\times\mathbf{H}_{\text{eff}}\right) + \frac{\alpha}{J_s}\left(\mathbf{J}\times\frac{\partial \mathbf{J}}{\partial t}\right) \qquad (6)$$

Equations (4) and (6) describe the physical path the system follow s towards equilibrium (Fig.1). The effective field $\mathbf{H}_{\text{eff}}$ which provides the torque acting on the magnetization is the negative functional derivative of the total magnetic Gibb's free energy. The first term in the right hand side of (4) and (6) describes the gyromagnetic precession, where γ is the gyromagnetic ratio of the free electron spin. The second term describes the dissipation of energy. It causes the magnetization to become aligned parallel to the effective field as the system proceeds towards equilibrium, the Gilbert damping parameter α is dimensionless. The dynamic micromagnetic simulation allows to describe the time evolution of the magnetization, if the damping parameter α is sufficiently known. For common ferromagnetic materials α is not constant and depends non linearly on the magnetisation.

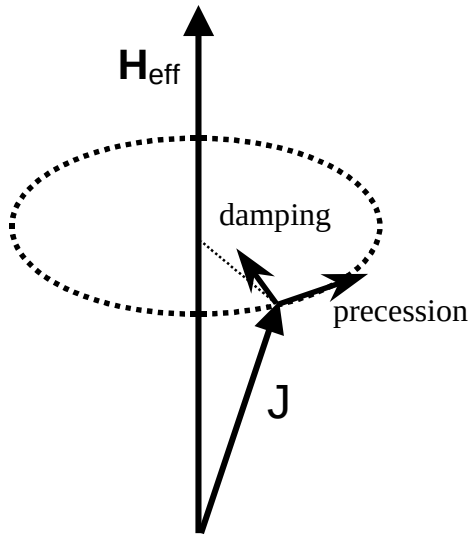

Fig.1. Damped gyromagnetic precession motion of a single magnetic polarization vector **J** towards the effective magnetic field $\mathbf{H}_{\text{eff}}$ according to the Gilbert equation of motion.

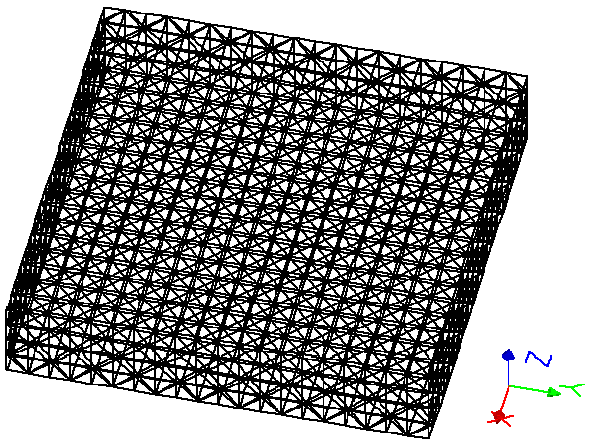

Fig.2. 3D finite element model of the square platelet with 2240 volume and 8000 surface tetrahedral elements used for the micromagnetic simulations.

The finite element method is a highly flexible tool to describe the interaction between microstructure and magnetization processes, since it is possible to incorporate the physical grain structure and intergranular phases and to adjust the finite element mesh according to the local magnetization. There are three main steps during the solution of a partial differential equation (PDE) with the finite element method. First, the domain, on which the PDE should be solved, is discretized into finite elements (Fig.2). Depending on the dimension of the problem these can be triangles, squares, or rectangles in two dimensions or tetrahedrons, cubes, or hexahedra for three dimensional problems. The solution of the PDE is approximated by piecewise continuous polynomials and the PDE is hereby discretized and split into a finite number of algebraic equations. When the components of the polarization vector are approximated by piecewise linear functions on the finite element mesh, the energy functional (1) and (2) reduces to an energy function with the nodal values of the vector components as unknowns. Its minimization with respect to the J_i at the nodal points, subject to the constraint $|\mathbf{J}|=J_s$, provides an equilibrium distribution of the polarization. To satisfy the constraint, the polarization is represented by polar coordinates. For the calculation of the demagnetizing field of mesoscopic or nanostructured magnets the magnetic scalar potential Ψ was calculated using a hybrid finite element/boundary element technique, which was originally proposed by Fredkin and Koehler [17]. The numerical integration of the Landau Lifshitz-Gilbert equation of motion provides the time resolved magnetization patterns during the reversal process. A Runge-Kutta method optimised for mildly-stiff differential equations [18] proved to be effective for the simulation using a regular finite element mesh and a Gilbert damping constant $\alpha \geq 0.2$. However, for an irregular mesh as required for triangular nanoelements and $\alpha = 0.1$ a time step smaller than 10 fs is required to obtain an accurate solution with the Runge-Kutta method. In this highly stiff regime, backward difference schemes allow much larger time steps and thus the required CPU time remains considerably smaller than with the Runge-Kutta method. Since the stiffness arises mainly from the exchange term, the demagnetising field can be treated explicitly and thus is updated after a time interval τ. During the time interval τ the Gilbert equation is integrated with a fixed demagnetising field using a higher order backward difference method. τ is taken to be inversely proportional to the maximum torque acting over the finite element mesh.

Micromagnetic simulation of $Ni_{80}Fe_{20}$ elements

In elements with zero magnetocrystalline anisotropy and in elements with random magneto-crystalline anisotropy magnetization reversal occurs by the formation and motion of vortices. Fig.3 compares the transient state during magnetization reversal of a $Ni_{80}Fe_{20}$ thin film element with rounded and slanted shapes. A spontaneous magnetic polarization of J_s = 1 T, an exchange constant of A = 13 pJ/m and zero magneto-crystalline anisotropy were assumed for the calculations. The extension of the tetrahedron elements was smaller or equal 5 nm which corresponds to the exchange length of the material. At first the remanent state of the elements with an extension of 100x50x10 nm^3 and a Gilbert damping constant of α=0.2 was calculated solving the Gilbert equation for zero applied field. The initial state for these calculations was a “C”-like domain

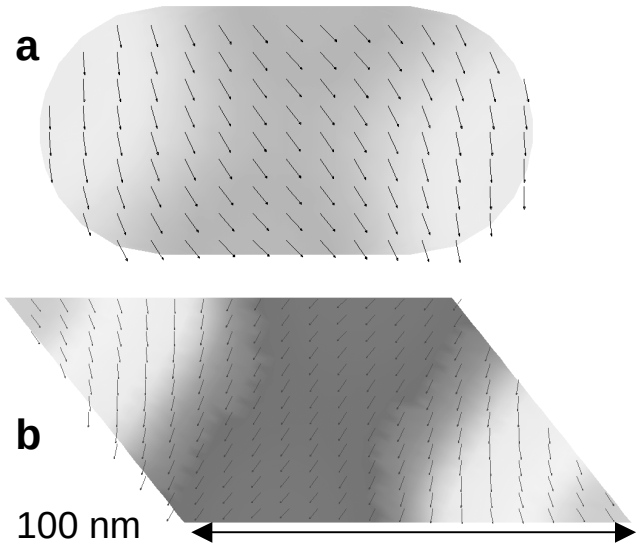

Fig.3: Polarization patterns during the switching of the NiFe elements with rounded (a) and slanted ends (b) assuming an extension of 100x50x10 nm^3 and a Gilbert damping constant of α = 0,2. H_{ext} = -80 kA/m is applied at an angle of 5° with respect to the long axis.

pattern. This procedure is believed to provide the minimum energy state for zero applied field. Then a reversed field of H_{ext} = 80 kA/m was applied at an angle of 5° with respect to the long axis of the particles.. Switching occurs by nonuniform rotation of the magnetization. The elements with slanted ends shows the fastest switching speed. As compared to the other elements the magnetization remains nearly uniform during the reversal process which reduces the switching time. After the rotation of the magnetization towards the direction of the applied field, the magnetization precesses around the direction of the effective field. As a consequence the magnetization as a function of time shows oscillations.

Submicron NiFe elements with an extension of 200x100x10 nm^3 switch well below 1 ns for an applied field of 80 kA/m, assuming a Gilbert damping constant of 0.1. The elements reverse by nonuniform rotation. Under the influence of an applied field, the magnetization starts to rotate near the ends, followed by the reversal of the centre. This process only requires about 0.1 ns. In what follows, the magnetization component parallel to the field direction shows oscillations which decay within a time of 0.4 ns. The excitation of spin waves originates from the gyromagnetic precession of the magnetization around the local effective field. A much faster decay of the oscillations occurs in elements with slanted ends, where surface charges cause in transverse magnetostatic field. The time required for the initial rotation of the magnetization decreases with decreasing damping constant and is independent of the element shape. However, the element shape influences the decay rate of the oscillations. A rapid decay is observed in elements with slanted ends. Magnetic nanoelements may be the basic structural units of future patterned media or magneto-electronic devices. The switching properties of acicular nano-elements significantly depend on the aspect ratio and shape of the ends. Pointed ends suppress the formation of end domains in the remanent magnetic state of NiFe nano-elements [19]. As a consequence the switching field decreases by a factor of 1/2 as compared to elements without blunt ends. Fig.4 shows the vortex formation at the blunt ends of an elongated, 200 nm wide, 1600 nm long and 26 nm thick NiFe element as magnetization reversal is initiated. In bars with one pointed end, the formation of the domains starts from the flat ends. Once vortices are formed, they easily break away from the edges causing the reversal of the entire element. Narrow elements with a width smaller than 200 nm remain in a nearly single domain state. Pointed ends suppress the formation of domains in NiFe elements.

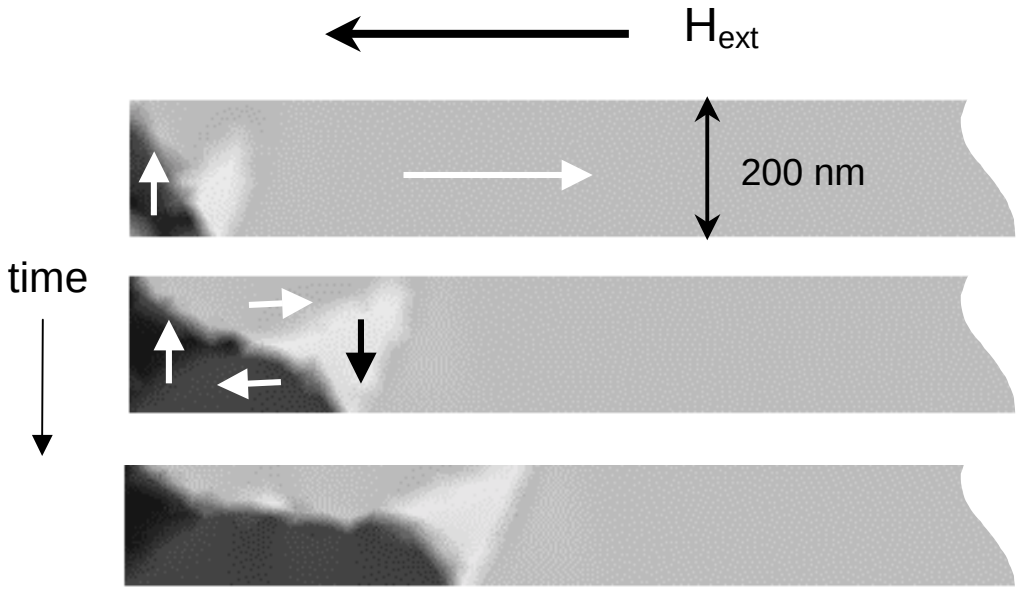

Fig.4. Vortex domain formation at an applied field of 19 kA/m for an elongated $Ni_{80}Fe_{20}$ nano- element with 1600x200x26 nm^3.

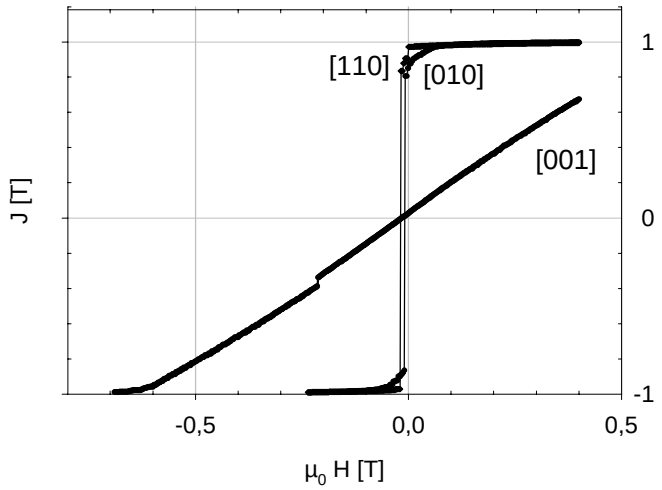

Fig. 5: Numerically calculated demagnetisation curves of a square NiFe platelet with 100 x 100 x 20 nm^3. The external field was applied parallel to the [001], [010] and [110] directions.

Differences of the demagnetising field which arise when the field is applied in different directions, lead to configurational anisotropy effects [20]. Platelet shaped elements show identical switching behaviour in different directions within the platelet plane. Inhomogeneous magnetization reversal processes become dominant with increasing element size ≥ 100 nm and strongly influence the switching behaviour. The numerical results show a strong influence of the size of cubic and platelet shaped $Ni_{80}Fe_{20}$ elements on the switching field. The calculated switching fields range from $\mu_0 H$=0.002 to 0.6 T for α=0.1. The nanomagnets were in the size range 10, 20, 40 and 100 nm for the edge length and in the thickness range 2, 4, 8 and 20 nm for the platelet shaped geometries (disc, square and triangular). The aspect ratio between edge length and thickness was kept constant. The nanomagnets were discretized into tetrahedral finite elements with a constant edge length of 5 nm and 2.5 nm for 10 nm edge length, respectively. The total number of the elements varied from 88 (10nm cube) to 44800 (100nm cube). The magnetic field was applied in certain crystallographic directions, and the calculations were started after saturation. The field was reduced in steps of $\mu_0 \Delta H$=0.002 T starting from $\mu_0 H$=0.4 T. Nanomagnets ≥ 40 nm show an inhomogeneous vortex-like magnetization structure during the reversal process. The resulting switching fields become independent of the direction of the magnetic field. In 100nm cubic elements the clear switching characteristic is replaced by inhomogeneous rotation of magnetization similar to the “hard direction” rotation. Platelet shaped elements also show this characteristic “hard direction” magnetization reversal perpendicular to the platelet surface. Only small differences of the switching behaviour in various directions within the platelet plane, such as [010], [110] for square elements (Fig.5) were found. Increasing the platelet size ≥ 100 nm the prompt switching changes to an inhomogeneous magnetization reversal resulting in a typical rounded demagnetisation curve (fig.5). The differences of the magnetization reversal modes are compared in Fig. 6 for square elements of different sizes.

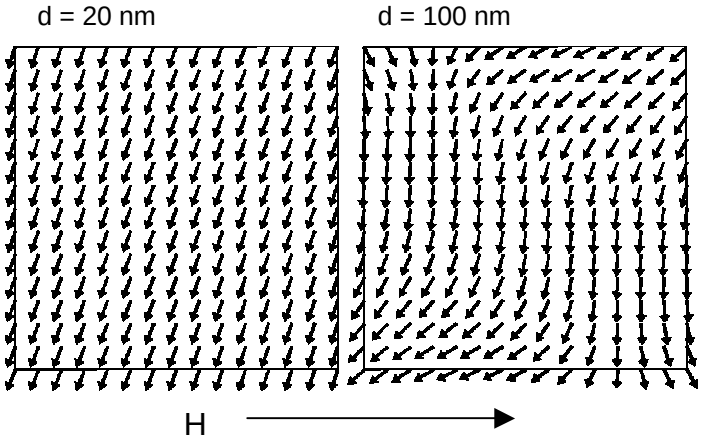

Fig. 6: Comparison of the transient magnetization states during the reversal of square elements of the size 20 x 20 x 4 nm^3 and 100 x 100 x 20 nm^3 with zero magnetocrystalline anisotropy under the influence of a constant reversed field of $\mu_0 H$= - 0.001 T parallel to the [010] direction.

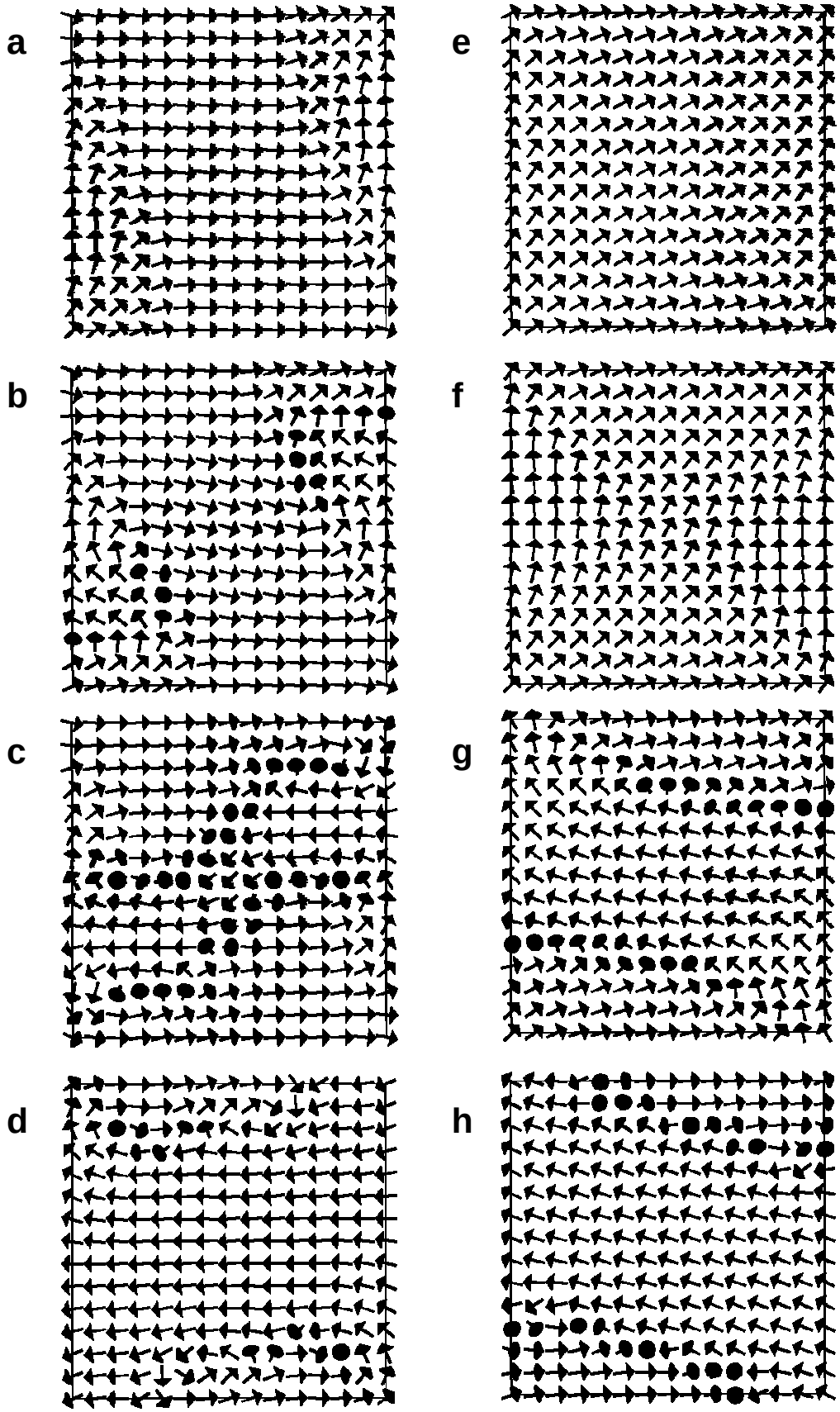

Fig. 7: Comparison of the transient magnetization states during the reversal of Co square elements of the size 100 x 100 x 20 nm^3 (a)-(d) under the influence of a constant reversed field of H_{ext}=280 kA/m parallel to the –y direction (e)-(h) under the influence of a rotating field of H_{ext}=280 kA/m with a frequency of 1 GHz applied in the (x,y)-plane

Micromagnetic simulation of Co elements under rotational external field

In mesoscopic and nanostructured magnets the switching fields and times which are in the order of nano- or picoseconds can be varied by the choice of the geometric shape of the magnets, the intrinsic properties and the orientation and strength of the applied field. Micromagnetic modelling of the magnetization reversal process show that the dynamics of the switching behaviour in a reversed field differs from the one in a rotating field, especially at high frequencies. We have used a 3D numerical micromagnetic model with tetrahedral finite elements with a constant edge length of 5 nm to study a thin Co square with dimensions 100 x 100 x 20 nm3 and the materials parameters J_s=1.76 T, K_1=4.5 x 10^5 J/m^3 and A=13 pJ/m. This simulation model combines a hybrid finite element/boundary element method for the magnetostatic field calculation with a BDF/GMRES method for the time integration of the Landau-Lifshitz-Gilbert equation of motion. The numerical results show that the Gilbert damping constant, α, which was varied between 0.1 and 0.02 drastically changes the reversal mode. The rotating magnetic field with a frequency of 1 GHz was applied in the (x,y)-plane and the calculations were started after saturation parallel to the y-direction (easy direction). The quasi-static simulation with $\mu_0\Delta H$=0.02 T showed that switching occurred at 0.2 H_A. Fig.7a-d shows the transient states during magnetization reversal at a constant reversed field of H_{ext}=280 kA/m parallel to the –y-direction. H_A is the anisotropy field value of the material. The element switches by nonuniform rotation at 0.7 ns for α=0.1. Fig.7e-h shows that the transient states during magnetization reversal in the high frequency rotational field (H_{rot}=280 kA/m / 1 GHz) differ from the ones of Fig.7a-d. Under the influence of the rotating field the magnetization starts to rotate near the ends, followed by the reversal of the centre. The results of the simulations show the influence of frequency and strength of rotating fields and unidirectional fields on switching field and time.

Transition to superparamagnetic behaviour

New experimental techniques allow spatially resolved measurements of magnetic structures of isolated magnetic particles. This leads to an increasing interest in the dynamics of the magnetisation reversal and its thermal stability of small magnetic particles down to nanometer regime. Small particles in the range of only few nanometers become superparamagnetic and thermally unstable. This limits the density of magnetic information storage materials. The understanding of the role of thermal activation for the dynamical behaviour of ferromagnetic particles is one of the most important subjects of modern micromagnetism. Thermal activation is introduced in the Landau-Lifshitz equation (4) by a stochastic thermal field H_{th}, which is added to the effective field [21]. The magnetization reversal process occurs in different reversal modes. In a particle with low anisotropy the polarization rotates incoherently. If the anisotropy is increased, it becomes favourable to form a nucleus with reversed magnetization. A droplet nucleates near the surface and expands until the magnetization is completely reversed. Fig.8 shows how the metastable lifetime τ decreases of a spherical particle with J_s= 0.5 T, A= 3.64 x 10^{-12} J/m, K_1= 2 x 10^5 J/m³, α=1 and a radius of 11.5 nm when the external field is increased.

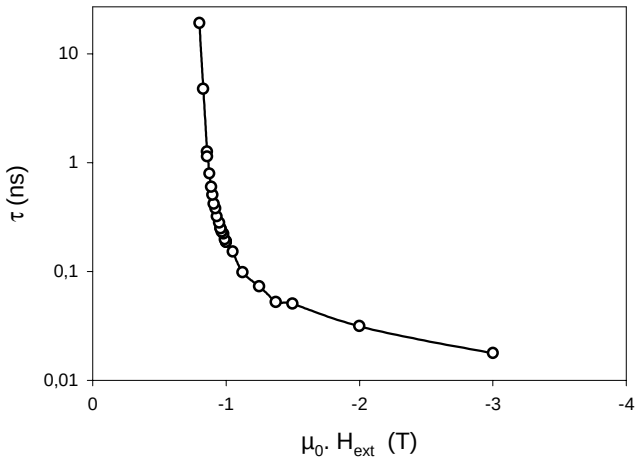

Fig.8. FE simulation of the dependence of the metastable lifetime on the external field for a small spherical particle with and a radius of 11.5 nm.

Summary

Micromagnetic finite element simulations show that the shape, the size, and the damping constant significantly influence the switching behaviour of thin film elements. Theoretical limits for remanence, coercive field, switching behaviour and other properties have successfully been calculated. Non uniform rotational processes play a significant role during magnetisation reversal. Using the hybrid finite element/boundary element method we investigated the influence of size and shape on the switching dynamics of mesoscopic or nanostructured $Ni_{80}Fe_{20}$ and Co elements. The numerical results show a strong influence of the element size on the switching behaviour. Configurational anisotropy effects were only observed in platelet shaped elements with magnetic field directions perpendicular to the platelet plane. Inhomogeneous magnetisation reversal processes become dominant with increasing element size $\geq$ 100 nm. The magnetisation reversal modes differ between rotational fields applied and unidirectional reversed fields. Incorporating thermally activated magnetization reversal will predict the upper limits of the switching frequency in thin film recording media.

ACKNOWLEDGMENT

This work was supported by the Austrian Science Fund (P13260-TEC).

REFERENCES

[1] Weller D. and Moser A. 1999 Thermal effect limits in ultrahigh-density magnetic recording IEEE Trans. Magn. 35 4423-4439.
[2] Richter H. J. 1999 Recent advances in the recording physics of thin-film media J. Phys.D: Applied Physics 32 R147-R168.
[3] Chou St.Y. 1997 Patterned magnetic nanostructures and quantized magnetic disks IEEE Trans Magn. 85 652-670.
[4] Frei E., H. Strikman S. and Treves D. 1957 Critical size and nucleation field of ideal ferromagnetic particles Phys. Rev. 106 446-455.
[5] Aharoni A. 1962 Theoretical search for domain nucleation Rev. Mod. Phys. 34 227-238.
[6] Nakatani Y., Uesaka Y. and N. Hayashi 1989 Direct solution of the Landau-Lifshitz-Gilbert Equation for micromagnetics Jpn. J. Appl. Phys. 28 2485-2507.
[7] Schabes M. E. and Bertram H. N. 1988 Magnetization processes in ferromagnetic cubes J. Applied Phys. 64 1347-1357.
[8] Koehler T. R. and Fredkin D. R. 1992 Finite element methods for micromagnetics IEEE Trans. Magn. 28 1239-1244.
[9] Victora R. H. 1988 Micromagnetic predictions for barium ferrite particles J. Appl. Phys. 63 3423-3428.
[10] Schabes M. E. 1991 Micromagnetic theory of non-uniform magnetization processes in magnetic recording particles J. Magn. Magn. Mater. 95 249-288.
[11] Yan Y. D. and Della Torre E. 1988 Reversal modes in fine particles J. de Physique C8 1813-1814.
[12] Schmidts H. F., Martinek G. and Kronmüller H. 1992 Recent progress in the interpretation of nucleation fields in hard magnetic particles J. Magn. Magn. Mater. 104-107 1119-1120.
[13] Fidler J. and Schrefl T. 2000 Micromagnetic modelling - the current state of the art, J. Phys. D 33 R135-R156.
[14] Aharoni A. 1991 Magnetostatic energy calculation IEEE Trans. Magn.. 27 3539-3547.
[15] Landau L. and Lifshitz E. 1935 On the theory of magnetic permeability in ferromagnetic bodies Physik. Z. Sowjetunion 8 153-169.
[16] Gilbert T. L. 1955 A Lagrangian formulation of gyromagnetic equation of the magnetization field Phys. Rev. 100 1243.
[17] Fredkin D. R. and Koehler T. R. 1990 Hybrid method for computing demagnetizing fields IEEE Trans. Magn., 26, 415-417.
[18] Sommeijer B.P., Shampine L.F. and Venwer J.G. 1998 RKC: an explicit solver for parabolic PDEs J. Comp.and Appl. Mathem. 66 315-326.
[19] Schrefl T., Fidler J., Kirk K.J. and Chapman J.N.1997 Domain structures and switching mechanisms in patterned magnetic elements J. Magn. Magn. Mat. 175 193-204.
[20] Cowburn R.P. 2000 Property variation with shape in magnetic nanoelements J. Phys. Dl 33 R1-R16.
[21] Scholz W., Schrefl T.and Fidler J. 2000 Micromagnetic simulation of thermally activated switching in fine particles J. Magn. Magn. Mater in press.